

# Predicting magnetic losses in HGO steel sheets under distorted induction waveform

N. Banu, M. Pasquale, and F. Fiorillo

<sup>1</sup>*Advanced Materials Metrology and Life Science Division, INRIM, Torino, Italy*

## ABSTRACT

1 We show that the magnetic losses of thin high-permeability grain-oriented Fe-Si sheets can be coherently  
2 assessed under sinusoidal and non-sinusoidal induction waveform by the analytical formulations provided by the  
3 Statistical Theory of Losses. Results are provided regarding the energy loss measured in 0,18 mm thick  
4 commercial sheets under sinusoidal induction and its change, for given peak polarization value  $J_p$ , with the  
5 distortion introduced by a third harmonic of defined amplitude  $J_{p3}$  and phase  $\varphi_3$  relationships with respect to the  
6 fundamental component. It is shown that accurate prediction of the 50 Hz losses at  $J_p = 1.7$  T for distortion  
7 generated by third harmonic peak polarization ratio  $J_{p3}/J_{p1} = 0.1, 0.2$ , and  $\varphi_3$  ranging between  $0^\circ$  and  $180^\circ$  can be  
8 made by the sole knowledge of the sinusoidal losses.

## I. INTRODUCTION

10  
11  
12 Pure sinusoidal regime is seldom achieved in magnetic cores, but their use in applications is still based on  
13 normative specifications and data sheets referring to the magnetic characterization performed under sinusoidal  
14 induction waveform. Novel applicative landscapes, accompanying the evolution of the electrical machines along  
15 the road to sustainable generation and transmission of the electrical energy, increasingly imply the integration of  
16 the magnetic cores with a driving electronic circuitry and make the working regimes of the cores generally  
17 depending on complex excitation waveforms. This is the case, for example, of grain-oriented (GO) steel cores  
18 used in turbogenerators and switched reluctance motors [1] [2], in solid state transformers [3] [4], and under the  
19 general circumstances occurring with power and distribution transformer cores supplying non-linear loads [5].

20 A meaningful approach to magnetic losses in steel sheets subjected to non-sinusoidal induction has been  
21 pursued in the literature by an array of methods. Empirical-phenomenological models, like the popular Steinmetz'  
22 model, its various extended/improved versions [6][7], and suitably modified classical formulas [8] have been  
23 proposed. Practical advantages in calculations, inherent to these models, are obscured by the feeble connection  
24 they have with the physical reality of the magnetization process. This is, on the contrary, the starting point of the  
25 Statistical Theory of Losses (STL) and the therein derived physical concept and formulation of the loss  
26 decomposition mechanism [9]. Originally developed for the prediction of the power loss in magnetic sheets  
27 subjected to constant rate of change of the magnetization, the STL was generalized later to sinusoidal and non-  
28 sinusoidal induction derivative [10] [11]. One obvious limitation of the STL approach is the eventual appearance  
29 of deep skin effect at high frequencies, which is accounted for either by making approximate phenomenological

30 corrections to the involved statistical parameters [12] or by solving the Maxwell's diffusion equation for the non-  
 31 linear medium [13]. This requires the identification of the magnetic constitutive equation of the material, which  
 32 is hysteretic in nature, and the use of numerical methods. It is shown that the matter can be simplified by  
 33 associating such equation with the normal magnetization curve [14].

34 For the specific case of GO sheets, criticism has been raised in the literature regarding the concept of loss  
 35 decomposition, on the ground that the classical eddy current losses may have a loose meaning for a material  
 36 endowed with a coarse domain structure [15] [16]. Consequently, it would be more appropriate to talk of dynamic  
 37 loss  $W_{\text{dyn}}(f)$ , without distinguishing between classical  $W_{\text{class}}(f)$  and excess loss  $W_{\text{exc}}(f)$  components. In this case,  
 38 however, one will resort again to a phenomenological formulation [16]. The physical modeling of the motion of  
 39 an ensemble of antiparallel domain walls (dws) under rated flux derivative, emulating the actual magnetization  
 40 process in the GO sheets, shows, however, that  $W_{\text{class}}(f)$  emerges as a natural effect of long-range eddy currents  
 41 and the statistics of the individual walls [9]. We can therefore justifiably write, whatever the case, the measured  
 42 energy loss at any frequency as

$$43 \quad W(f) = W_{\text{hyst}} + W_{\text{class}}(f) + W_{\text{exc}}(f), \quad (1)$$

44 where the hysteresis (quasi-static) loss component is, as far as deep skin effect is not involved, independent of  
 45 frequency. The present experiments, performed in thin high-permeability GO sheets, endowed with slab-like  
 46 domain structure, fit excellently with the STL. It is shown that, starting from the STL-guided decomposition of  
 47  $W(f)$ , measured from DC to 200 Hz under sinusoidal flux, we can predict with high accuracy the evolution of the  
 48 50 Hz energy loss following different degrees of distortions, as obtained with the introduction of a third harmonic  
 49 of variable phase and amplitude.

## 50 II. EXPERIMENTAL PROCEDURE. -1

51 The magnetic losses and hysteresis loops were measured for defined  $J_p = 1.7$  T in 0.18 mm thick Epstein  
 52 strips of commercial HGO Fe-Si, according to the IEC 60404-2 standard (Epstein test frame). Sinusoidal and  
 53 non-sinusoidal flux waveforms were imposed by digital feedback, implemented in the operation of a wattmeter-  
 54 hysteresisgraph setup [17]. This is endowed with a 12-bit LeCroy HDO 4054 for signal acquisition, with the  
 55 primary winding supplied by an NF HSA 4014 high-speed power amplifier driven by an Agilent 33220A arbitrary  
 56 function generator. The energy loss was first measured up to 200 Hz with sinusoidal induction. Fig. 1a shows the  
 57 measured  $W(f)$  curve, together with its components. Once the classical loss is calculated by the standard equation  
 58

$$59 \quad W_{\text{class}}(f) = \left(\frac{\pi^2}{8\delta}\right)\sigma d^2 J_p^2 f \quad , \quad [\text{J/kg}] \quad (2)$$

60 where  $\sigma$  and  $\delta$  are the conductivity and the mass density of the material and  $d$  is the sheet thickness, the quantity  
 61  $W(f) - W_{\text{class}}(f) = W_{\text{hyst}} + W_{\text{exc}}(f)$  is plotted against  $f^{1/2}$  (Fig. 1b). For the investigated HGO alloy it is  $\sigma = 2.083 \cdot 10^6$   
 62  $\Omega^{-1}\text{m}^{-1}$  and  $\delta = 7650$  kg/m<sup>3</sup>. As predicted by the STL, a linear dependence of this quantity on  $f^{1/2}$  is observed,  
 63 vindicating the related physical model for the case of coarse domain structure. It is also an obvious confirmation  
 64 of the absence of skin effect. The measurements were then performed at 50 Hz by introducing a third harmonic  
 65  $J_3(t)$  of peak amplitude  $J_{3p}$  in the ratio  $R = J_{3p}/J_{1p} = 0.1$  and  $R = 0.2$  to the fundamental harmonic and relative  
 66 phase shift  $\varphi_3$  ranging between  $0^\circ$  and  $180^\circ$ . For any phase shift,  $J_{1p}$  and  $J_{3p}$  were adjusted in order to maintain  $J_p$   
 67  $= 1.7$  T everywhere. Examples of imposed  $J(t)$  and  $dJ/dt$  non-sinusoidal waveforms

$$68 \quad 69 \quad J(t) = J_1 \cos \omega t - R J_1 \cos(3\omega t + \varphi_3) \quad \frac{dJ(t)}{dt} = -\omega J_1 \sin \omega t + 3\omega R J_1 \sin(3\omega t + \varphi_3) \quad (3)$$

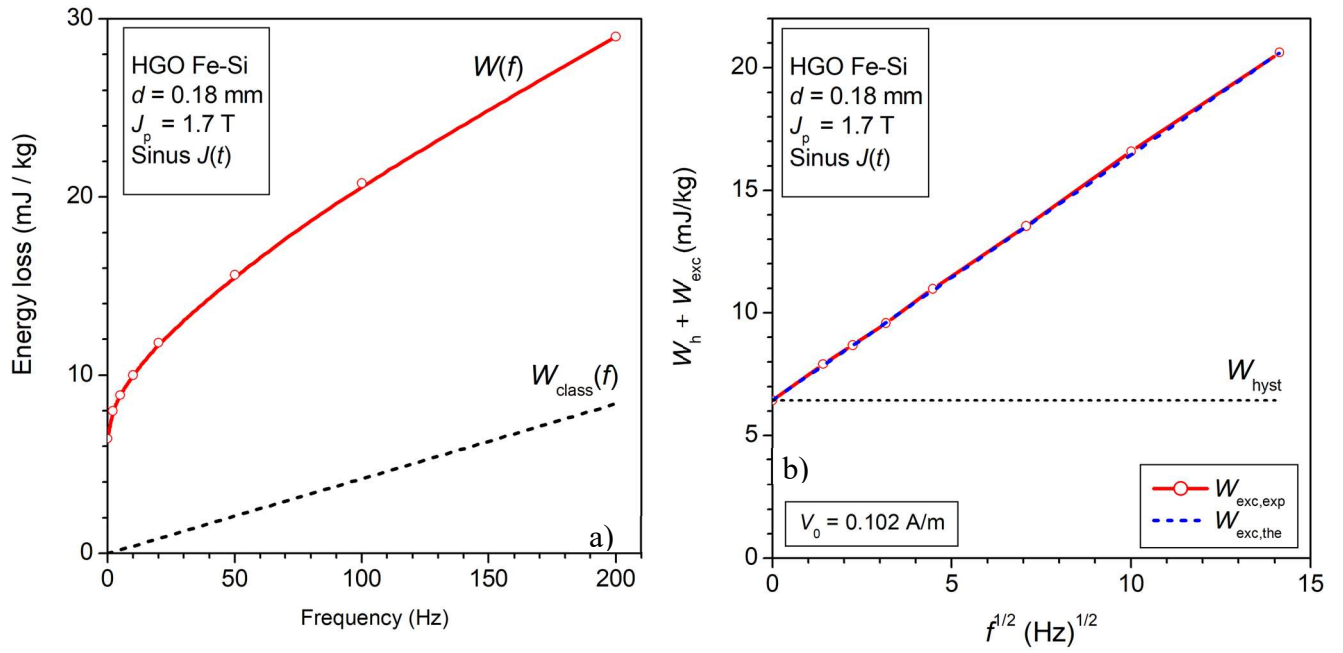


Fig. 1 – a) Energy loss versus frequency measured in a 0.18 mm thick HGO Fe-Si sheet under sinusoidal polarization of peak value  $J_p = 1.7$  T. The classical loss component  $W_{\text{class}}$  is calculated with (1). b) The quantity  $W(f) - W_{\text{class}}(f) = W_{\text{hyst}} + W_{\text{exc}}(f)$  is plotted versus  $f^{1/2}$ . Following the STL, this behavior is interpreted in terms of hysteresis loss  $W_{\text{hyst}}$  independent of frequency and  $W_{\text{exc}}(f) \propto f^{1/2}$ .

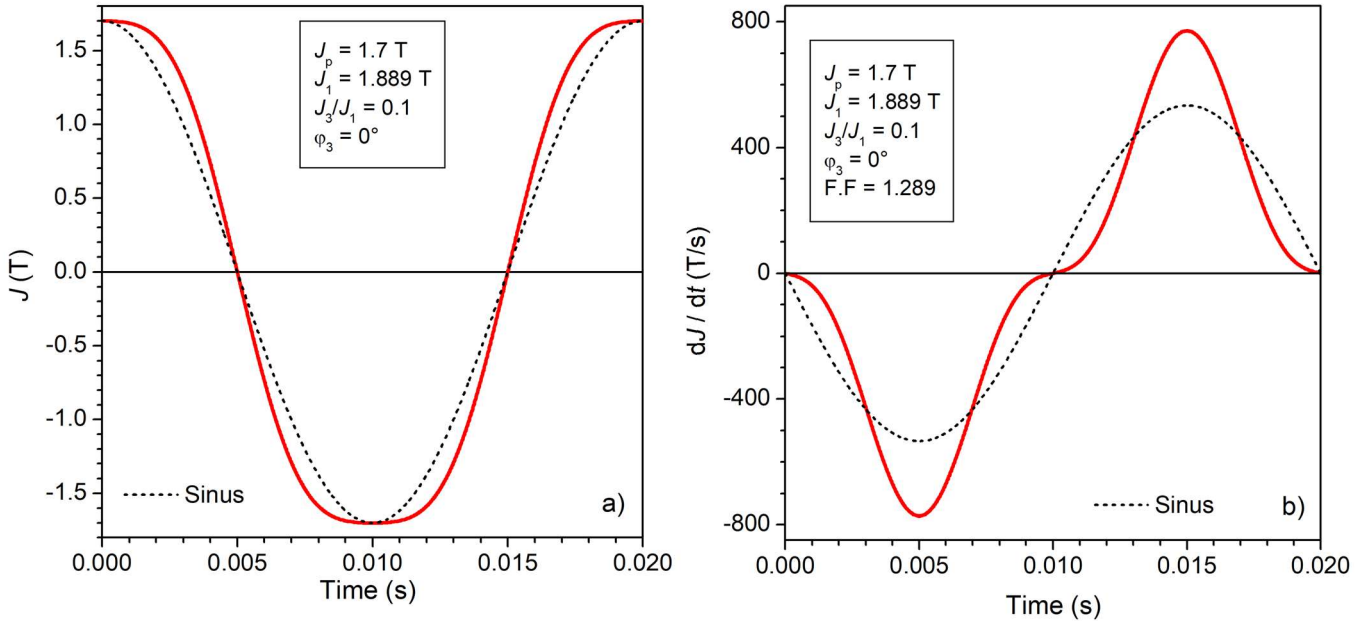


Fig. 2 – a) Polarization waveform of peak polarization  $J_p = 1.7$  T composed of a fundamental harmonic of amplitude  $J_{p1}$  and a third harmonic of amplitude  $J_{p3}$  in the ratio  $R = J_{p3}/J_{p1} = 0.1$  and phase shift  $\varphi_3 = 0$  (see Eq. (3)). The dashed line belongs to the sinusoidal  $J(t)$  of equal  $J_p$  value. b) Time derivative of  $J(t)$ .

70 are provided in Figs. 2 and 3. The whole set of investigated  $J(t)$  waveforms is shown in Table 1. Fig. 4 illustrates  
 71 the experimental evolution of the hysteresis loops at 50 Hz and  $J_p = 1.7$  T under different degrees of distortion of  
 72  $J(t)$ . It is noted in Fig. 4 that the condition  $R = 0.2$  and  $\varphi_3 = 2^\circ$ , leads to the generation of a minor loop of local  
 73 peak amplitude  $\Delta J_p = 0.07$  T.

74

### 75 III. ENERGY LOSS vs. WAVEFORM DISTORTION AND ITS PREDICTION

76 The  $W(f)$  behavior under sinusoidal polarization  $J(t)$  shown in Fig. 1 is assessed by means of loss  
 77 decomposition, where  $W_{\text{class}}(f)$  is calculated by Eq. (1) and the quantity  $W(f) - W_{\text{class}}(f) = W_{\text{hyst}} + W_{\text{exc}}(f)$ , plotted  
 78 against  $f^{1/2}$ , permits one to straightforwardly separate  $W_{\text{hyst}}$  and  $W_{\text{exc}}(f)$ . The latter perfectly fits into the theoretical  
 79 prediction by the STL, according to the equation

$$81 \quad W_{\text{exc}}(J_p, f) = \left(\frac{8.76}{\delta}\right) \sqrt{\sigma G S V_0} (J_p) f J_p^{3/2}, \quad [\text{J/kg}] \quad (4)$$

82  
 83 where  $G = 0.1356$ ,  $S$  is the cross-sectional area of the sample under test, and the parameter  $V_0$ , having the  
 84 dimension of a magnetic field, is a statistical parameter, to be found by equating (4) with the experimental  $W_{\text{exc}}(f)$   
 85 in Fig. 1b.  $V_0$  bears a precise physical meaning, because it relates to the statistics of the local coercive fields  
 86 involved with the dw motion. We find, in the present case of HGO sheets, the value  $V_0(J_p = 1.7 \text{ T}) = 0.102 \text{ A/m}$ .

87 A basic physical assumption lying behind Eq. (4) is the possibility do define the instantaneous power loss

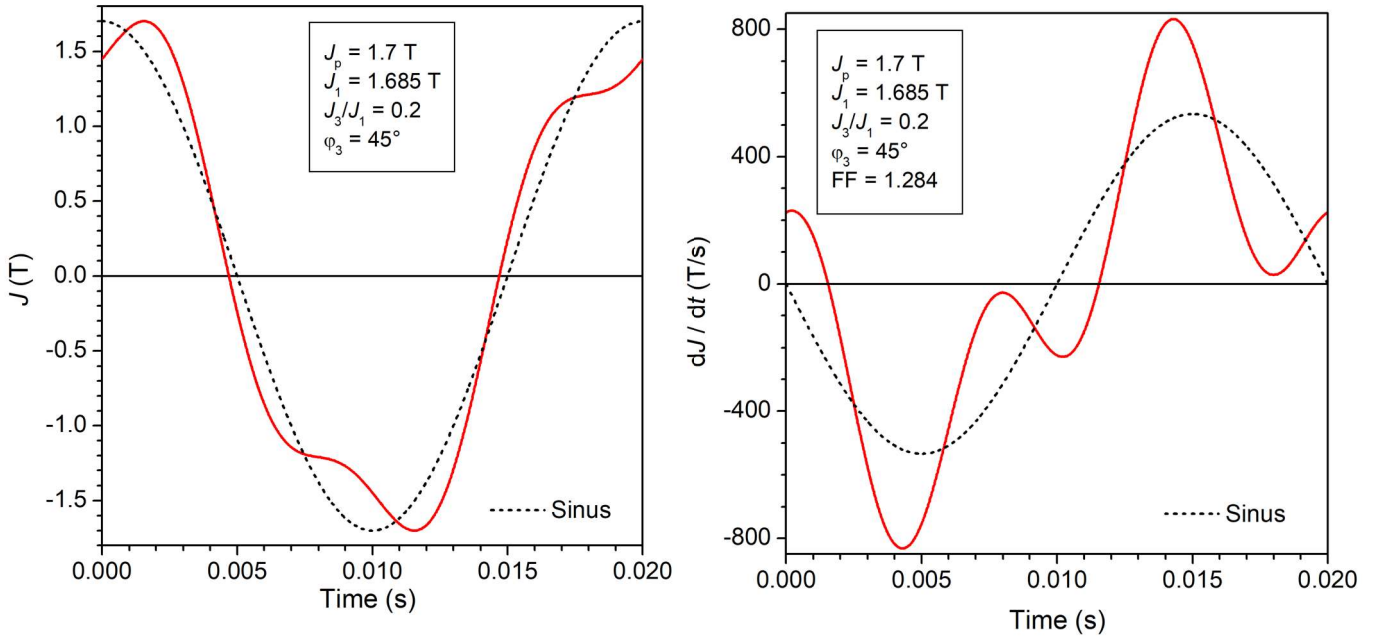


Fig. 3 –As in Fig. 2 for  $R = J_{p3}/J_{p1} = 0.2$  and phase shift  $\varphi_3 = 45^\circ$ .

88 for all the components [9] [10]. This permits us to find the average power loss, that is, the energy loss per cycle,  
 89 by integrating the instantaneous loss over the period. As far as the distortion is not engendering local minima of  
 90 the polarization along the period  $T$ , the hysteresis loss is independent of the polarization waveform. Under these  
 91 circumstances, we need to calculate  $W_{\text{class}}(f)$  and  $W_{\text{exc}}(f)$  as a function of the specifically envisaged  $J(t)$ . We  
 92 therefore write, according to the definition of instantaneous classical power loss

$$94 \quad W_{\text{class}}(J_p, f) = \frac{\sigma d^2}{12\delta} \cdot \int_0^T \left(\frac{dJ}{dt}\right)^2 dt . \quad [\text{J/kg}] \quad (5)$$

95  
 96 We calculate, at the same time, the excess loss by a similar integration [11]

$$98 \quad W_{\text{exc}}(J_p, f) = \left(\frac{1}{\delta}\right) \sqrt{\sigma G S V_0} \cdot \int_0^T \left|\frac{dJ}{dt}\right|^{3/2} dt . \quad [\text{J/kg}] \quad (6)$$

99

100 It is immediately obtained that, for  $J(t) = J_p \cos \omega t$ , Eq. (4) is retrieved. For all the harmonic combinations  
 101 illustrated in Table 1, Eqs. (5) and (6) have been calculated and added to  $W_{\text{hyst}}$  in Eq. (1). The comparison between  
 102 measured and predicted loss figures is provided in Table 2. Fig. 6 equivalently shows the dependence of the  
 103 experimental and theoretically predicted energy losses as a function of the parameter  $\varphi_3$ , normalized to the energy  
 104 loss value measured under sinusoidal  $J(t)$ .  
 105

Table 1 – The investigated set of  $J(t)$  waveforms made of fundamental  $J_1(t)$  and third harmonic  $J_3(t)$  components, according to  $J(t) = J_1 \cos \omega t - R J_3 \cos(3\omega t + \varphi_3)$ . The harmonics are in the ratio  $R = J_{3p} / J_{1p}$  and are phase shifted by the angle  $\varphi_3$ . The peak value of the resulting waveform is induction is always  $J_p = 1.7$  T.

106  
107  
108  
109  
110  
111  
112  
113  
114  
115  
116  
117

$R = J_{3p}/J_{1p}$	$\varphi_3$ (°)	$J_p$ (T)	$J_{1p}$ (T)	$J_{3p}$ (T)	Form Factor $dJ/dt$
0.1	0	1.7	1.889	0.1889	1.289
0.1	30	1.7	1.807	0.1807	1.233
0.1	45	1.7	1.759	0.1759	1.200
0.1	60	1.7	1.714	0.1714	1.169
0.1	90	1.7	1.639	0.1639	1.118
0.1	150	1.7	1.555	0.1555	1.061
0.1	180	1.7	1.545	0.1545	1.054
0.2	2	1.7	1.937	0.387	1.375
0.2	30	1.7	1.76	0.352	1.337
0.2	45	1.7	1.685	0.337	1.284
0.2	60	1.7	1.622	0.3244	1.236
0.2	90	1.7	1.527	0.3056	1.164
0.2	150	1.7	1.428	0.2856	1.088
0.2	180	1.7	1.417	0.2834	1.080

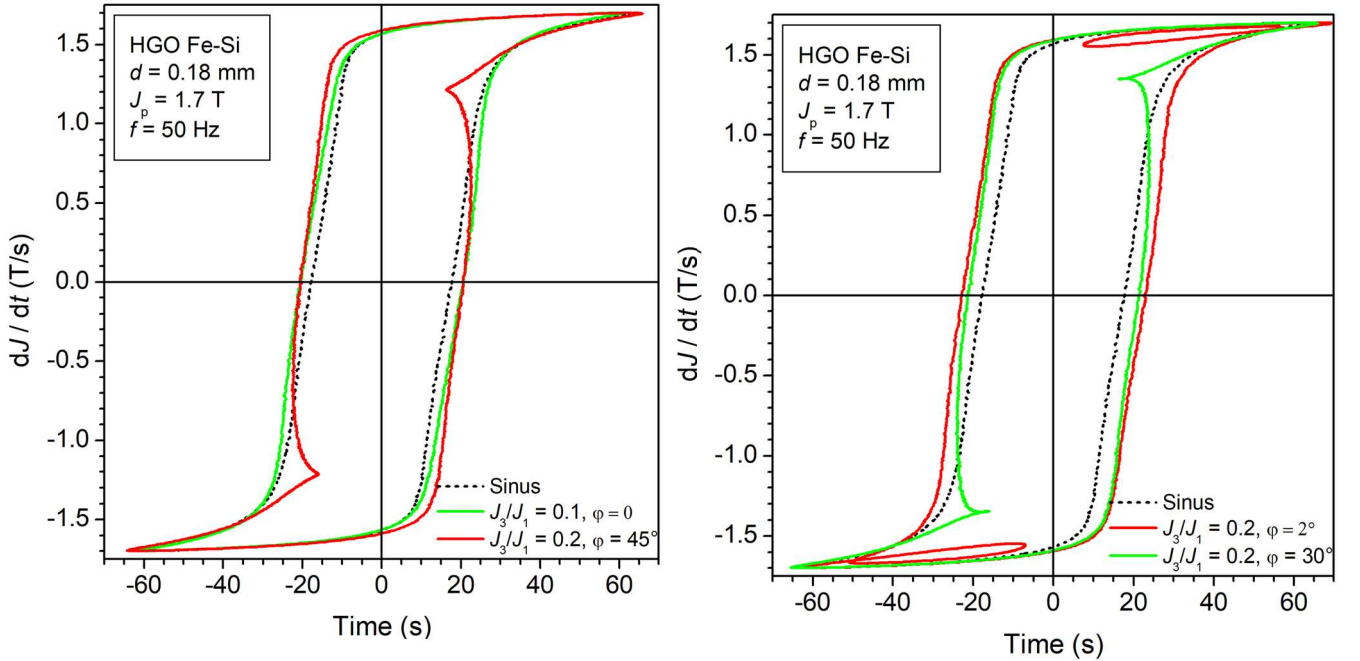


Fig. 4 – Hysteresis loops measured at 50 Hz under sinusoidal and non-sinusoidal polarization  $J(t)$  for  $J_p = 1.7$  T. To note the formation of a minor loop for the combination  $J_{3p}/J_{1p} = 0.2$  and phase shift  $\varphi_3 = 2^\circ$ . In this case we need to account for a small additional contribution to  $W_{\text{hyst}}$ .

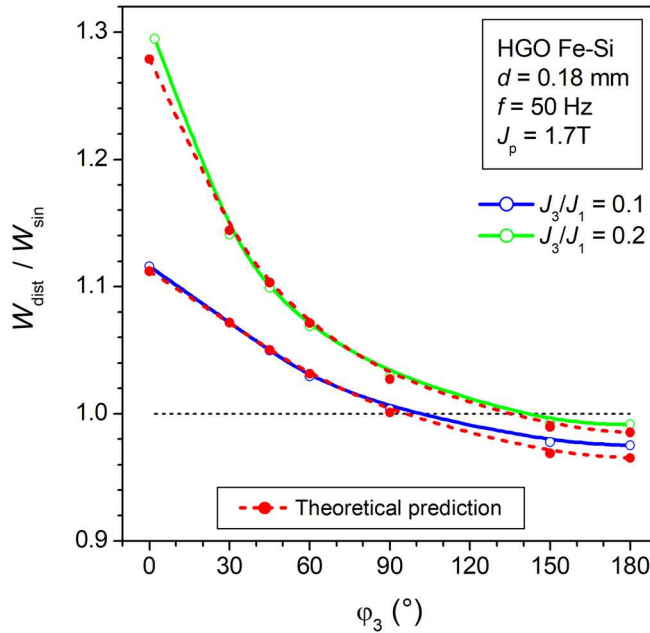


Fig. 5 - Evolution with the degree of distortion of the 50 Hz energy loss measured at  $J_p = 1.7$  T in the HGO Fe-Si sheets (solid lines) and its prediction by use of Eqs. (5) (6), and (1) (dashed lines).

Table 2 – Measured and predicted 50 Hz energy losses at 50 Hz at  $J_p = 1.7$  T versus the parameters identifying the distorted polarization waveform. The loss figure measured under sinusoidal  $J(t)$  is 16.44 mJ/kg. The difference between the measured and predicted loss figures is of the order of the measuring uncertainty.

118

$\varphi_3$ (°)	$J_3/J_1$	$W_{\text{meas}}$ (mJ/kg)	$W_{\text{calc}}$ (mJ/kg)	$J_3/J_1$	$W_{\text{meas}}$ (mJ/kg)	$W_{\text{calc}}$ (mJ/kg)
0	0.1	17.45	17.392	---	---	---
2	---	---	---	0.2	20.25	20
30	0.1	16.7646	16.762	0.2	17.845	17.897
45	0.1	16.42	16.427	0.2	17.1895	17.252
60	0.1	16.1	16.133	0.2	16.7165	16.756
90	0.1	15.7	15.655	0.2	16.1095	16.064
150	0.1	15.29	15.152	0.2	15.525	15.482
180	0.1	15.25	15.098	0.2	15.509	15.411

123

## CONCLUSIONS

124

The energy losses of thin high-permeability grain-oriented sheets have been measured at 50 Hz under various degrees of distortion introduced, for given peak polarization value  $J_p = 1,7$  T, by a third harmonic component of variable amplitude and phase shift. It is shown that, starting from the experimental results obtained under sinusoidal magnetization, the Statistical Theory of Losses permits one to accurately predict the behavior of the loss figure imposed by the evolution of the magnetization waveform. The theory permits one, in particular, to separately calculate the effect of distortion on the classical and the excess loss components, with the hysteresis (quasi-static) loss remaining unaffected, but for the case where a local minimum of the  $J(t)$  waveform (additional minor hysteresis loop) enters into play. The degree of accuracy of the calculated loss figures is comparable with the experimental measuring uncertainty.

133

## ACKNOWLEDGMENTS

134

This research work was carried out in the framework of the project 19ENG06 HEFMAG, This project was funded by the EMPIR programme, co-financed by the Participating States and from the European Union's Horizon 2020 research and innovation programme.

135

136

137

- 139 [1] L. Millan Mirabal, O. Messall, A. Benabou, Y. Le Menach, L. Chevallier, J. Korecki, J. Roger, J. Ducreux,  
140 "Iron Loss Modeling of Grain Oriented Electrical Steels in FEM Simulation Environment," *IEEE Trans. Magn.*  
141 **58**, article n° 6300805 (2022). doi: 10.1109/TMAG.2021.3097586
- 142 [2] Y. Matsuo, T. Higuchi, T. Abe, Y. Miyamoto and M. Ohto, "Characteristics of a novel segment type switched  
143 reluctance motor using grain-oriented electric steel," *2011 International Conference on Electrical Machines and*  
144 *Systems*, 2011, pp. 1-4, doi: 10.1109/ICEMS.2011.6073428.
- 145 [3] X. She, "Review of solid state transformer technologies and their applications in power distribution systems,"  
146 *IEEE J. Em. Sel. Topics Pow. Electr.* **1**, pp. 186-198 (2013). Doi:10.1109/JESTPE.2013.2277917.
- 147 [4] H. Ichou, D. Roger, M. Rossi, T. Belgrand, and R. Lemaître, Assessment of a grain-oriented wound core  
148 transformer for solid state converter," *J. Magn. Magn. Mater.* **504**, article n° 166658 (2020).  
149 doi: 10.1016/j.jmmm.2020.1666658.
- 150 [5] D.M. Said and K.M. Nor, "Effects of harmonics on distribution transformers," Proc. **2008** Australasian  
151 Universities Power Engineering Conference (AUPEC '08), 2008.
- 152 [6] J. Li, T. Abdallah, and C. Sullivan, "Improved calculation of core loss with nonsinusoidal waveforms," *Proc.*  
153 *IEEE Ind. Appl. Soc. Ann. Meet.*, Oct. 2001, pp. 2203–2210. doi: [10.1109/IAS.2001.955931](https://doi.org/10.1109/IAS.2001.955931).
- 154 [7] S. Barg, K. Ammous, H. Mejibri, and A. Ammous, "An improved empirical formulation for magnetic core  
155 losses estimation under nonsinusoidal induction," *IEEE Trans. Power. Electron.* **32**, pp. 2146–2154 (2017). Mar.  
156 2017. 10.1109/TPEL.2016.2555359.
- 157 [8] S. Yanase, H. Kimata, Y. Okazaki, and S. Hashi, "A simple predicting method for magnetic losses of electrical  
158 steel sheets under arbitrary induction waveform," *IEEE Trans. Magn.* **41**, pp. 4365-4367 (2005). doi:  
159 10.1109/TMAG.2021.3097586.
- 160 [9] G. Bertotti, *Hysteresis in Magnetism*. San Diego, CA, USA: Academic Press, 1998, pp. 391–430.
- 161 [10] F. Fiorillo and A. Novikov, "An improved approach to power losses in magnetic laminations under non-  
162 sinusoidal induction waveform.", *IEEE Transactions on Magnetics* **26**, pp. 2904 – 2910 (1990). doi:  
163 [10.1109/20.104905](https://doi.org/10.1109/20.104905).
- 164 [11] E. Barbisio, F. Fiorillo, and C. Ragusa, "Predicting loss in magnetic steels under arbitrary induction  
165 waveform and with minor hysteresis loops," *IEEE Trans. Magn.* **40** pp. 1810-1819 (2004). doi:  
166 10.1109/TMAG.2004.830510.
- 167 [12] Z. Zhao and X. Hu, "Modified loss separation in FeSi laminations under arbitrary distorted flux," *AIP Adv.*  
168 **10**, article n° 085222 (2020). doi: 10.1063/5.0020789.
- 169 [13] L. Dupre, O. Bottauscio, M. Chiampi, M. Repetto, and J. Melkebeek, "Modeling of electromagnetic  
170 phenomena in soft magnetic materials under unidirectional time periodic flux excitations," *IEEE Trans. Magn.*  
171 **35**, pp. 4171-4184, 1999. doi: 10.1109/20.799065.
- 172 [14] A. Magni, A. Sola, O. de la Barrière, E. Ferrara, L. Martino, C. Ragusa, C. Appino, and F. Fiorillo,  
173 "Domain structure and energy losses up to 10 kHz in grain-oriented Fe-Si sheets," *AIP Adv.*, **11** Article n°  
174 015220 (2021). doi.org/10.1063/9.0000184.
- 175 [15] S.E. Zirka, Y.I. Moroz, P. Marketos, A.J. Moses, D.C. Jiles, T. Matsuo, *IEEE Trans. Magn.* **44**, pp. 2113-  
176 2126 (2008). doi:10.1109/TMAG.2008.2000662.
- 177 [16] S.E. Zirka, Y.I. Moroz, S. Steentjes, K. Hameyer, K. Chwastek, S. Zurek, and R.G. Harrison, "Dynamic  
178 magnetization models for soft ferromagnetic materials with coarse and fine domain structures," *J. Magn. Magn.*  
179 *Mater.*, **394**, pp. 229-236 (2015), doi: 10.1016/j.jmmm.2015.06.082.
- 180 [17] F. Fiorillo, *Measurement and Characterization of Magnetic Materials* (Academic-Elsevier, San Diego, CA,  
181 2004).  
182  
183  
184  
185